Electronic Structure of Localized Si Dangling-Bond Defects by Tunneling Spectroscopy

R. J. Hamers and J. E. Demuth
IBM T. J. Watson Research Center, Yorktown Heights, New York 10598
(Received 20 October 1987)

Scanning tunneling microscopy is used to determine the atomic structure, charge state, and electronic energy spectrum of isolated Si dangling-bond defects at the Al/Si(111) surface. Si adatoms substituting for Al in the first atomic layer give rise to a dangling-bond defect state near −0.4 eV which is strongly localized in space. Tunneling spectra and local band-bending measurements are inconsistent with simple one-electron band theory and demonstrate the importance of many-electron effects.

PACS numbers: 73.20.Hb, 61.16.Di

The atomic geometry, charge state, and energy spectrum of localized defect states at metal-semiconductor interfaces have been subjects of considerable experimental and theoretical interest because of their possible role in Fermi-level pinning and Schottky-barrier formation.[1-5] Tunneling microscopy has allowed us to examine the topology and observe defects and irregularities at surfaces. In all previous tunneling measurements, one-electron band theory has been shown to provide adequate explanation of the observed features. Yet, for a localized defect state, this one-electron band picture is expected to break down as the spatial extent of the defect wave functions becomes comparable to the size of an individual atom.

In this paper we use scanning tunneling microscopy (STM) to study naturally occurring point defects at a surface. We identify the atomic origin of these states and show the correlation between our tunneling spectroscopy results and previous ultraviolet photoemission spectroscopy results. The results are inconsistent with simple "one-electron" band models and demonstrate that many-electron effects can strongly affect the electronic state density of localized point defects at surfaces.

The scanning tunneling microscope used in this study was described previously.[6] We have measured simultaneously both normal topographic images and constant-separation I-V curves (at each location) via the current-imaging tunneling spectroscopy method.[7] Silicon wafers (6-mΩ-cm Sb doped and 5-mΩ-cm B doped) were cleaned as described previously[7] to produce well-ordered Si(111)-(7×7) surfaces. The sample was then again heated to 875 K and aluminum was deposited from a filament source. Al coverages were monitored with a quartz-crystal monitor which was calibrated with use of Rutherford backscattering. Low-energy electron diffraction was used to identify and characterize the Al overlayer as a function of temperature and coverage and found to be in close agreement with early work by Lander and Morrison.[8] The deposition of $\frac{1}{3}$ monolayer Al onto a Si(111)-(7×7) surface at 875 K routinely produced well-ordered Si(111)-($\sqrt{3}\times\sqrt{3}$)Al.

Figure 1 shows STM topographic images of the Al/Si(111) surface taken at −2- and +2-V sample bias (1-nA tunneling current) on the n-type material; images taken on p-type material were essentially identical. At positive sample bias [Fig. 1(a), +2-V sample bias], characteristic defects (marked "S") are observed which appear to be lower by ≃1 Å than the nascent $\sqrt{3}$-Al unit cells (marked "I" for ideal), while still having an obvious protrusion at their center. At negative sample bias [Fig. 1(b), −2 V] these same defects appear to be nearly 1 Å *higher* than the plane of the $\sqrt{3}$-Al surface. *Vacancy* de-

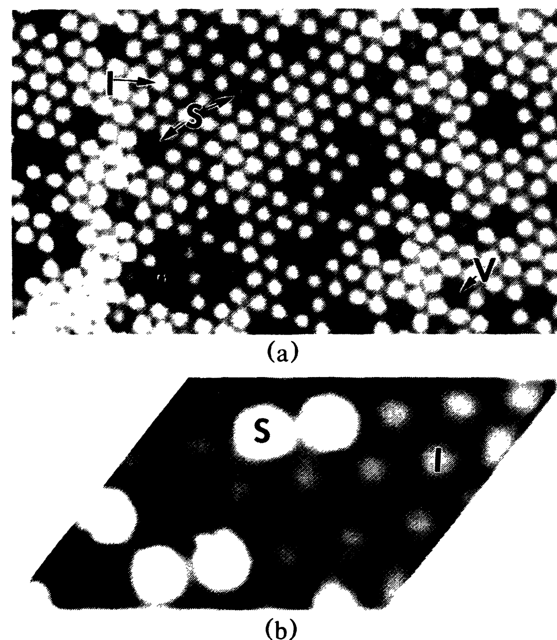

FIG. 1. STM topographic images of nominally Si(111)-($\sqrt{3}\times\sqrt{3}$) surface at (a) positive (+2 V) and (b) negative (−2 V) sample bias. White regions are high and dark regions low. Ideal $\sqrt{3}$-Al unit cells are indicated by I. Si substitutional defects (marked S) appear as darker cells with bright center at positive sample bias (a) and bright spots at negative bias (b). (a) also contains a few *vacancy* defects, marked V, which do *not* have a bright spot in the center.

fects (marked "V" in Fig. 1) are also (infrequently) observed. Vacancies appear $\simeq 2$ Å lower than the surrounding $\sqrt{3}$-Al regions at both positive and negative bias and do *not* have a protrusion in the center. The characteristic topographic height variations observed on these surfaces are depicted quantitatively in Fig. 2, which show corrugation profiles along $\langle 1\bar{1}0\rangle$ over ideal $\sqrt{3}$-Al unit cells and both S and V defects under specified conditions.

The dependence of the S-type defects on Al coverage shows that they arise from Si adatoms (instead of Al adatoms) on a Si(111) substrate. For $\Theta_{\rm Al} < \frac{1}{3}$ monolayer (ML), STM images show the surface to be a $\sqrt{3}$ overlayer of interspersed Al and Si adatoms in varying proportions. At $\Theta \simeq \frac{1}{3}$ ML (as in Fig. 1), a few percent of the surface is Si adatoms, while for $\Theta > \frac{1}{3}$ ML a $(\sqrt{7}\times\sqrt{7})$ structure begins to form but the remaining $\sqrt{3}$ regions have only a small number of silicon adatoms.

In order to study the energy spectrum of these defects, the tunneling I-V characteristics were analyzed on S-type defect sites and on $\sqrt{3}$-Al overlayer atoms (I). The I-V results are presented as plots of $(V/I)dI/dV$ vs V, which is effectively a density of states normalized to unity at $V=0$.[9-12] Figure 3 shows such plots for 1-Å^2 areas centered above an I atom in an ideal Si(111)-$(\sqrt{3}\times\sqrt{3})$Al unit cell [3(a)] and at a typical S defect [3(b)]. On the "normal" Si(111)-$(\sqrt{3}\times\sqrt{3})$Al unit cells, we observe a surface-state band gap, with pronounced peaks in $(V/I)dI/dV$ at -1.5 and $+0.9$ eV.

At the S-type defects, we find several changes. Most noticeable is the presence of a a new state whose density of states peaks near -0.4 eV and contributes significant state density from $E_{\rm F}$ to $\simeq 1$ eV below $E_{\rm F}$. The strong occupied band which for the ideal $\sqrt{3}$-Al structure was located near -1.5 eV also appears to be shifted in energy, reaching a maximum near -1.7 eV. The measured state density has a *minimum* at $E_{\rm F}$ and again increases for $E > E_{\rm F}$, with a small peak visible at $+0.9$ eV, identical to that on the surrounding Al adatoms.

These tunneling spectroscopy observations can be directly related to previous photoemission studies of $\sqrt{3}$-Al,[15-18] which have observed a defect state at -0.4 eV with a coverage dependence similar to that observed here under nearly identical preparation conditions. Our STM results show that this -0.4-eV state originates at isolated Si substitutional defects within the perfect $\sqrt{3}$ structure and is not associated with domain boundaries.[16] Defect states near this same energy have also been reported for $\sqrt{3}$-Ga/Si(111) (Ref. 17) at -0.4 eV and for $\sqrt{3}$-In/Si(111) (Ref. 13) at -0.25 eV. This suggests that the Si substitutional defect observed here for Al/Si(111) is common to most group-III metals on Si(111), where similar bonding geometries (and, hence, defect structures) are expected.

The STM results consistently demonstrate that these Si substitutional defects are very strongly localized, having only weak interactions with other top-layer atoms.

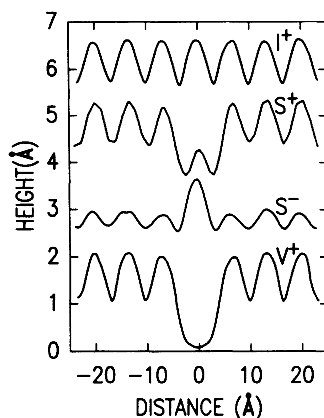

FIG. 2. STM corrugation profiles along $\langle 1\bar{1}0\rangle$ on defected $\sqrt{3}$-Al surfaces under specified conditions. In the lowest three curves, each profile passes over six ideal $\sqrt{3}$-Al adatoms and over one nonideal cell located at the center. I$^+$: ideal $\sqrt{3}$-Al region, +2-V sample bias. S$^+$: substitutional defect, +2-V sample bias. S$^-$: substitutional defect, -2-V sample bias. V$^+$: vacancy defect, +2-V sample bias.

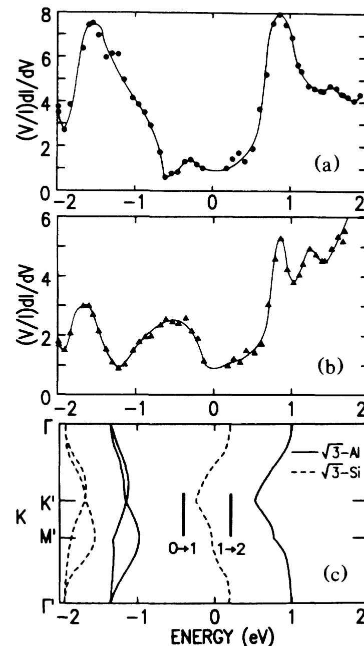

FIG. 3. Tunneling density-of-states measurements taken above (a) normal and (b) defected unit cells. The quantity $(V/I)dI/dV$ is normalized to unity at $V=0$. (c) Northrup's calculated band structures for extended $\sqrt{3}$-Si and $\sqrt{3}$-Al surfaces (after Refs. 13 and 14). The solid bars near -0.4 and $+0.2$ eV schematically indicate the energies and occupation numbers of the transitions observed in deep-level transient spectroscopy measurements of the P_b center (from Refs. 1 and 2).

For example, measurements of the apparent height of Si adatoms in individual defects and two- to three-atom clusters of defects relative to the "ideal" $\sqrt{3}$-Al surface show only small changes as a function of cluster size. Tunneling spectroscopy measurements show no significant difference between the state density at Al adatoms in ideal regions and those adjacent to the Si defects. Finally, angle-resolved ultraviolet photoemission spectroscopy measurements show less than 0.1 eV dispersion of this state across the entire surface Brillouin zone.[16,18] These measurements show that the nature of the S defect is independent of the surrounding adatoms, so that it can be thought of as an isolated Si adatom. Such strong localization likely results from the large separation (6.65 Å) between nearest neighbors in the surface plane.

For an sp^3-hybridized Si adatom, one-electron band theories[14] predict that three electrons are accounted for in bonding the Si adatom to the substrate, while the fourth electron lies in a partially occupied p_z-like "dangling-bond" state. In the single-electron approximation, a partially occupied dangling-bond state must lie at the Fermi energy. This is the case in Si(111)-(7×7), where Si-adatom dangling bonds interact and form a half-occupied band at E_F. Likewise, self-consistent pseudopotential calculations by Northrup[14] predict a half-filled band for Si adatoms atop Si(111) in a $(\sqrt{3}\times\sqrt{3})$ geometry. However, our tunneling spectroscopy results show that the state density on the Si adatoms peaks well below E_F. This shift of state density from E_F to −0.4 eV is significant because it implies that the total number of electrons localized at the defect, given by the state density integrated up to E_F, changes correspondingly. The observed −0.4-eV energy suggests that the dangling-bond state is completely occupied and the defect is negatively charged.

In order to determine experimentally the charge on these defects, detailed measurements were made of the STM corrugation profiles shown in Fig. 2. The charging of defects is expected to produce band bending in the surrounding region which can be observed in the STM topographs.[11] Such band bending should be particularly apparent here, since the ideal $\sqrt{3}$-Al surface has a large surface-state band gap. However, the corrugation profiles show no evidence of such band bending around the defects on either *n*-type (as in Fig. 2) or *p*-type material. Band bending *is* observed around some *other* defects (usually at domain boundaries), giving rise to apparent height changes of several angstroms and decaying away with a lateral decay length of ≃15 Å, in good agreement with the screening length expected from the bulk doping. This demonstrates that while we have the sensitivity to detect band bending associated with charged defects, it is absent around these S defects. This leads us to conclude that the S defects are *not* charged, but are electrically neutral. The absence of significant charge transfer from Al to Si adatoms is further supported by surface core-level measurements[5,15] and theoretical studies[14,19] which show that Al adsorption involves minimal charge transfer so that both Al and Si adatoms are *covalently* bonded to the Si(111) surface.

The one-electron prediction of a half-filled p_z-like state at the Fermi energy contradicts our experimental observation of a *minimum* in the measured state density at E_F. The origin of this discrepancy is the failure of one-electron band theories to include Coulomb and correlation effects which become important for highly localized states. The Coulomb energy associated with the confinement of one or two electrons into an atomic-sized defect can be quite large, so that the dangling-bond band is more correctly described by three discrete charge states depending on whether the number of electrons at the defect, *n*, is 0, 1, or 2. The theory of such localized defects has been extensively treated by Mott[20] and Hubbard,[21] and a similar model has been proposed by Duke and Ford[22] to explain the observed surface-state band gap on Si(111)-(1×1). For highly *localized* defects, many-electron calculations show that the $n=1$ (neutral) charge state gives rise to a *bimodal* state distribution,[21] with a minimum at E_F, in agreement with our experimental observations. This state distribution gives rise to two electrical levels—a donor level corresponding to the $n=1\rightarrow n=0$ transition, and an acceptor corresponding to the $n=1\rightarrow n=2$ transition. Since the physical process of the removal of an electron from the defect corresponds to the $n=1\rightarrow n=0$ transition, the −0.4-eV energy measured in both STM and photoemission corresponds to the energy of the donor level relative to E_F. Above E_F it is difficult to identify the corresponding Mott-Hubbard acceptor level because of overlap with the pronounced p_z-like state on the Al adatoms. However, the minimum at E_F is clearly observed.

The STM results indicate that $U_{eff}>0.4$ eV. This value is consistent with previous studies of similar Si dangling-bond defects. Theoretical calculations by Fowler[23] for an isolated Si dangling bond predict $U_{eff}=0.4$–0.5 eV. Experimental measurements of Si dangling-bond defects in α-SiH (Stuke[24]) and the well-known P_b center at the Si-SiO_2 interface[1,2] show U_{eff} of 0.35 and 0.7 eV, respectively. Given the strong geometric similarity between those dangling-bond defects and the one at the Al/Si(111) interface observed here, the value of $U_{eff}>0.4$ eV obtained from our tunneling spectroscopy measurements is quite reasonable.

Finally, the midgap states introduced by these Si adatoms are expected to play an important role in the determination of the surface Fermi-level position. This is demonstrated by our spectroscopic measurements, which show no shift in the Fermi energy between *n*- and *p*-type samples, and is consistent with calculations by Zur, McGill, and Smith[4] which predict that a dangling-bond concentration of approximately 10^{13} cm^{-2} is sufficient to

pin the surface Fermi level independent of the bulk doping, because movement of E_F is easily prevented by the charging of a small number of defects.

In summary, we have used STM to identify and characterize Si dangling-bond defects. We demonstrate that the electron states associated with these defects are strongly localized in space. We find that one-electron band theory is insufficient to understand the nature of these localized surface defects and that many-electron effects must be taken into account.

The authors would like to acknowledge many useful discussions with Ph. Avouris, N. Lang, S. Pantelides, J. Tersoff, and A. Williams. This work is supported in part by the U.S. Office of Naval Research.

---

[1]N. M. Johnson, D. K. Biegelsen, M. D. Moyer, S. T. Chang, E. H. Poindexter, and P. J. Caplan, Appl. Phys. Lett. **43**, 562 (1983).

[2]N. M. Johnson, W. B. Jackson, and M. D. Moyer, Phys. Rev. B **31**, 1194 (1985).

[3]W. E. Spicer, P. R. Skeath, C. Y. Su, and P. Chye, Phys. Rev. Lett. **44**, 420 (1980).

[4]A. Zur, T. C. McGill, and D. L. Smith, Phys. Rev. B **28**, 2060 (1983).

[5]L. J. Brillson, A. D. Katnani, M. Kelly, and G. Margaritondo, J. Vac. Sci. Technol. A **2**, 551 (1984).

[6]J. E. Demuth, R. J. Hamers, R. M. Tromp, and M. E. Welland, J. Vac. Sci. Technol. A **4**, 1320 (1986).

[7]R. J. Hamers, R. M. Tromp, and J. E. Demuth, Phys. Rev. Lett. **56**, 1972 (1986).

[8]J. J. Lander and J. Morrison, Surf. Sci. **2**, 553 (1964).

[9]R. J. Hamers, to be published.

[10]J. A. Stroscio, R. M. Feenstra, and A. P. Fein, Phys. Rev. Lett. **57**, 2579 (1986).

[11]J. A. Stroscio, R. M. Feenstra, and A. P. Fein, Phys. Rev. Lett. **58**, 1668 (1987).

[12]N. Lang, Phys. Rev. B **34**, 5947 (1986).

[13]J. M. Nicholls, P. Mårtensson, G. V. Hansson, and J. E. Northrup, Phys. Rev. B **32**, 1333 (1985).

[14]J. E. Northrup, Phys. Rev. Lett. **53**, 683 (1984).

[15]G. V. Hansson, R. Z. Bachrach, R. S. Bauer, and P. Chiaradia, Phys. Rev. Lett. **46**, 1033 (1981).

[16]T. Kinoshita, S. Kono, and T. Sagawa, Phys. Rev. B **32**, 2714 (1985).

[17]T. Kinoshita, S. Kono, and T. Sagawa, Solid State Commun. **56**, 681 (1985).

[18]R. I. G. Uhrberg, G. V. Hansson, J. M. Nicholls, P. E. S. Persson, and S. A. Flodstrom, Phys. Rev. B **31**, 3805 (1985).

[19]H. Nagayoshi, in *Dynamical Processes and Ordering on Solid Surfaces,* edited by A. Yoshimori and M. Tsukoda, Springer Series in Solid-State Sciences Vol. 59 (Springer-Verlag, New York, 1985).

[20]N. F. Mott, *Metal-Insulator Transitions* (Taylor and Francis, London, 1974).

[21]J. Hubbard, Proc. Roy. Soc. London A **276**, 238 (1963).

[22]C. B. Duke and W. K. Ford, Surf. Sci. **111**, L685 (1981).

[23]W. B. Fowler and R. J. Elliott, Phys. Rev. B **34**, 5525 (1986).

[24]J. Stuke, Philos. Mag. B **52**, 225 (1985).

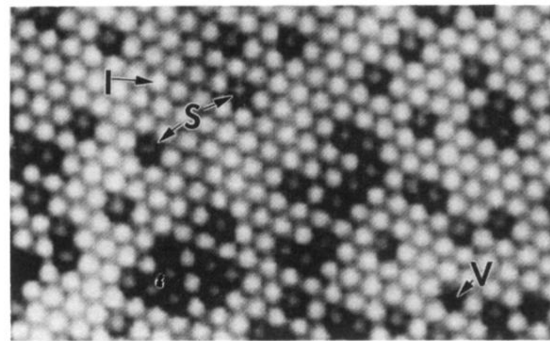

(a)

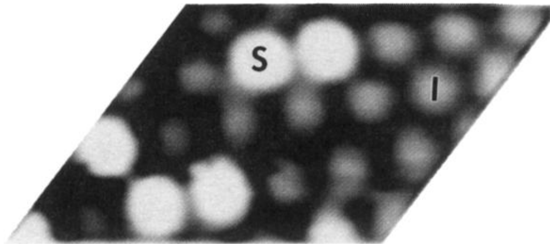

(b)

FIG. 1. STM topographic images of nominally Si(111)-($\sqrt{3}\times\sqrt{3}$) surface at (a) positive (+2 V) and (b) negative (−2 V) sample bias. White regions are high and dark regions low. Ideal $\sqrt{3}$-Al unit cells are indicated by I. Si substitutional defects (marked S) appear as darker cells with bright center at positive sample bias (a) and bright spots at negative bias (b). (a) also contains a few *vacancy* defects, marked V, which do *not* have a bright spot in the center.